

Preliminary Analysis of Skywave Effects on MF DGNSS R-Mode Signals During Daytime and Nighttime

Suhui Jeong

*School of Integrated Technology
Yonsei University
Incheon, Republic of Korea
ssuhui@yonsei.ac.kr*

Pyo-Woong Son*

*Korea Research Institute of Ships and Ocean Engineering
Daejeon, Republic of Korea
pwson@kriso.re.kr
* Corresponding author*

Abstract—Accurate positioning, navigation, and timing (PNT) performance are prerequisites for several technologies today. In a marine environment, it is difficult to visually identify one's position accurately, leading to safety concerns. Currently, PNT information is provided mainly from Global Navigation Satellite Systems (GNSS); however, it is vulnerable to radio frequency interference, spoofing, and ionospheric anomaly. Therefore, research on a backup system is needed. Ranging Mode (R-Mode), a terrestrial integrated navigation system, is being investigated for use in a marine environment. R-Mode is a positioning technology that integrates terrestrial signals of opportunity such as medium frequency (MF) differential GNSS (DGNSS), very high frequency (VHF) automatic identification system (AIS), and enhanced long-range navigation (eLoran) signals. Previous studies in Europe show that signals in the MF band differ greatly in accuracy between daytime and nighttime. This difference is primarily caused by skywave. In this study, the MF DGNSS R-Mode signal transmitted from Chungju, Korea was received in Daesan and Daejeon, Korea. The skywave effect during daytime and nighttime was compared and investigated. In addition, the continuous wave intensity of the R-Mode signal was increased during the nighttime to compare its effect on the measurement accuracy.

Index Terms—MF DGNSS R-Mode, skywave, PNT

I. INTRODUCTION

Accurate positioning, navigation, and timing (PNT) information is one of the essential requirements of current technologies, such as telecommunications, transportation, port logistics, and numerous location-based applications. Owing to the lack of visually identifiable features in the marine environment, it is difficult to identify location accurately; therefore, safety concerns dictate the importance of PNT information. Accurate PNT information is necessary for contemporary marine technologies such as autonomous ships. PNT information are currently obtained, both on land and at sea, mainly using Global Navigation Satellite Systems (GNSS) [1]–[4]. However, the GNSS system relies on satellite transmission; hence, the received signal is very weak. Therefore, it is vulnerable to artificial interference such as jamming and spoofing [5]–[8] or ionospheric anomaly [9], [10]. Several backup navigation systems have been studied [11]–[23]. A

navigation system using “Signals of Opportunity” (SoOp), is a system that utilizes current broadcast radio frequency (RF) signals for navigation, either directly or after certain changes [24]–[27]. Research on “Ranging Mode” (R-Mode) navigation systems using medium frequency (MF) signals for differential GNSS (DGNSS) transmission and very high frequency (VHF) signals for automatic identification system (AIS) transmission as SoOp is being conducted in the maritime sector [28]–[34]. R-Mode investigation using three different configurations of MF DGNSS, VHF AIS, and enhanced long-range navigation (eLoran) [35]–[39] are also being conducted [29]. Currently, the R-Mode technology development in Korea is underway [40].

The maritime DGNSS ground reference station transmits GNSS correction information by minimum shift keying (MSK) modulation of a signal in the 285–325 kHz frequency band. In the R-Mode, continuous waves (CW) can be added to the existing MF DGNSS signals to provide positioning capability. Validation of the MF R-Mode in the North Sea area revealed a significant difference in accuracy, approximately 10 times, between daytime and nighttime positioning [30]. The major cause of error was identified as skywave. According to [30], skywaves occur after sunset and have a significant effect on the positioning accuracy at night. Unlike the pulse signal of eLoran, the CW signal of MF R-Mode is continuous signal, making it difficult to separate the direct signal and skywave [31].

In this study, we analyzed the positioning accuracy of MF DGNSS R-Mode in daytime and nighttime based on preliminary data from the MF R-Mode testbed in Korea under development. For the analysis, the data were collected in Daesan and Daejeon, Korea, and the received signals were transmitted from Chungju, Korea.

II. MF R-MODE SKYWAVE MODEL

An MF DGNSS reference station transmits a signal by modulating the GNSS correction information using MSK in the 285–325 kHz range. When the amplitude of the signal is A , the bit interval is T , carrier frequency is f_c , phase offset is

TABLE I
RMS DISTANCE ERROR (M) OF CW1 AND CW2 IN DAYTIME AND NIGHTTIME (DAEJEON)

	Daytime	Nighttime
CW1	320095	427741
CW2	320060	427741

TABLE II
RMS DISTANCE ERROR (M) OF CW1 AND CW2 IN DAYTIME AND NIGHTTIME (DAESAN)

	Daytime	Nighttime
CW1	229602	343526
CW2	229618	343399

Φ , and bit stream is ± 1 , the MSK signal is expressed by (1) in [41].

$$s_{\text{msk}}(t) = A \cos \left(2\pi f_c t \pm \frac{\pi t}{2T} + \Phi \right). \quad (1)$$

One of the existing MF DGNSS R-Mode implementations adds two continuous waves at the frequencies of $f_c \pm 250$ Hz to the MF DGNSS signal for ranging. With amplitude B and phase offset Φ , the continuous wave signals can be expressed as [42]

$$\begin{aligned} s_{CW1}(t) &= B_{CW1} \cos(2\pi(f_c - 250)t + \Phi_{CW1}) \\ s_{CW2}(t) &= B_{CW2} \cos(2\pi(f_c + 250)t + \Phi_{CW2}). \end{aligned} \quad (2)$$

The combined signal of (1) and (2) is transmitted as an MF R-Mode signal and is represented by the following equation:

$$\begin{aligned} s(t) &= s_{\text{msk}}(t) + s_{CW1}(t) + s_{CW2}(t) \\ &= A \cos \left(2\pi f_c t \pm \frac{\pi t}{2T} + \Phi \right) \\ &\quad + B_{CW1} \cos(2\pi(f_c - 250)t + \Phi_{CW1}) \\ &\quad + B_{CW2} \cos(2\pi(f_c + 250)t + \Phi_{CW2}). \end{aligned} \quad (3)$$

The receiver receives a groundwave, where the transmitted signal propagates along the ground propagation path, and a skywave that is reflected by the ionosphere. The skywave can be modeled as a time-delayed and amplitude-scaled version of the groundwave [30]. According to the results of [30], the R-Mode positioning error's lower bound was 10 m during daytime in the North Sea area; however, it was 100 m at nighttime, which is a 10 times reduction. Skywaves begin at sunset and last until sunrise; thus, adversely affecting the nighttime performance. The skywave model with time delay t_d and attenuation factor α is expressed as follows [30]:

$$r(t) = s(t) + \alpha s(t - t_d). \quad (4)$$

III. MEASUREMENT DATA ANALYSIS

The R-Mode signal transmitter for our measurement campaign was in Chungju, Korea, and the receiver was in Daesan and Daejeon, Korea. The receiver used for this study is the Serco's "MFR-1a Medium Frequency R-Mode Receiver," which was also used in [32]. Signals were simultaneously collected from two receivers. The receiver provided the distance

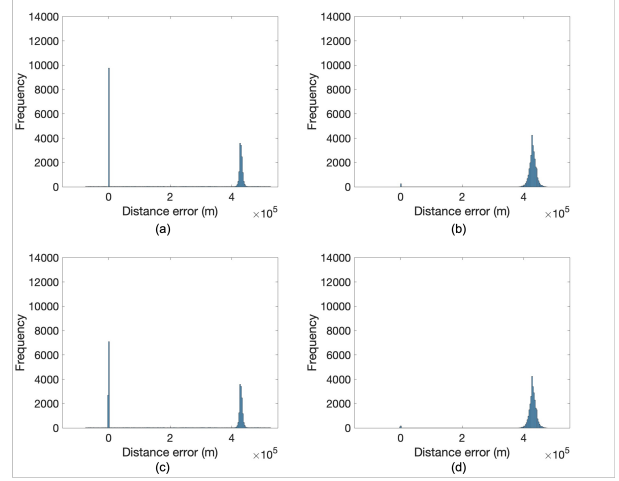


Fig. 1. Distance error distribution during (a) daytime and (b) nighttime with CW1 signal, and (c) daytime and (d) nighttime with CW2 signal in Daejeon, Korea.

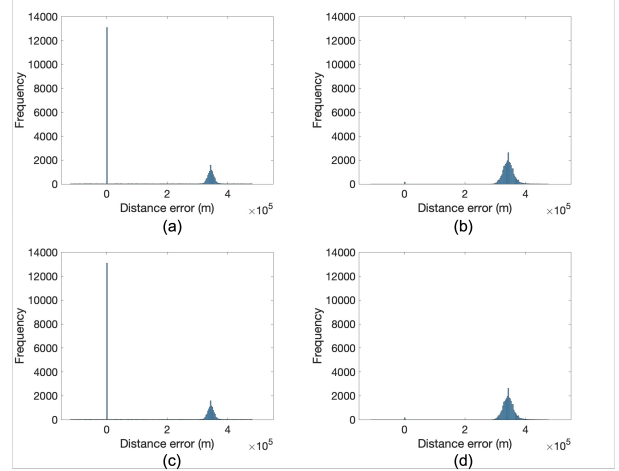


Fig. 2. Distance error distribution during (a) daytime and (b) nighttime with CW1 signal, and (c) daytime and (d) nighttime with CW2 signal in Daesan, Korea.

data used for the analysis. The transmission center frequency f_c was 318 kHz, and CW1 and CW2 were 318.25 kHz and 317.75 kHz, respectively. Daytime refers to the time from 6 am to 6 pm, and the nighttime refers to the time from 6 pm to 6 am the next morning. The data was collected from 1:30 pm on April 21, 2022 to 11:30 am the next day. To investigate the effect of increased signal intensity on positioning accuracy, the intensity of CW signals was increased for three hours from 9 pm to 12 am.

The received data was analyzed in two parts. First, the distribution of distance measurement errors between daytime and nighttime was compared to determine the skywave effect at night. Second, data with increased CW signal intensity was compared with data without the increase from the nighttime measurements. The received signal with the signal-to-noise ratio (SNR) of 7 dB or greater was used for the analysis,

which is the minimum standard for a maritime DGNSS beacon receiver prescribed by the International Electrotechnical Commission (IEC) [43].

A. Daytime and Nighttime Comparison of MF DGNSS R-Mode Accuracy

To equalize the amount of daytime and nighttime data, daytime data from 1:25 pm to 6 pm and 6 am to 9 am the next day, and nighttime data from 6 pm to 9 pm and 1:25 am to 6 am were used. The root mean square (RMS) errors of the distance measurements provided by the Serco receiver during daytime and nighttime in Daejeon and Daesan are listed in Tables I and II, respectively. The histograms of the error distributions in Daejeon and Daesan are shown in Figs. 1 and 2, respectively.

Regarding the distribution of distance errors in both Daesan and Daejeon data, it is evident that there is a high frequency of small distance errors during the daytime; however, at nighttime, the error is very large as it is rarely measured accurately. The distance error distributions around the very large errors in Figs. 1 and 2 are likely caused by wrong integer ambiguity resolution in the receiver. Thus, the RMS distance error values in Tables I and II do not reflect the potential performance of the MF R-Mode with a correct integer value. Nevertheless, the different error distributions between daytime and nighttime are clearly shown in Figs. 1 and 2. Unlike [30], where accuracy was measured at sea, in the testbed of our study, the propagation path was along the ground, which causes additional errors.

B. MF DGNSS R-Mode Accuracy Analysis with Modified and Unmodified Signals

From 9 pm to 12 am, the intensity of the CW signal was increased. This signal with the increased intensity is called “modified signal” in this paper, and the original signal without the increased intensity is called “unmodified signal.” This three-hour data with the modified signal was compared with another three-hour data with the unmodified signal collected from 12 am to 3 am.

Tables III and IV lists the average SNR of the modified and unmodified signals according to CW1 and CW2. Similar to Section III-A, we compared the distance error distributions measured in Daejeon and Daesan. The results are shown in Figs. 3 and 4. The distributions of the modified signal cases are closer to the zero, which implies more accurate distance measurements. Because a CW signal is used to measure distance, the stronger the received CW signal, the more accurate the measured distance. This suggests the possibility of increasing the nighttime accuracy by adjusting the CW signal strength.

IV. CONCLUSION

In this study, we analyzed the signals collected in Daesan and Daejeon to investigate the skywave effects on the MF R-Mode. The analysis was conducted by comparing the distance error distribution based on time of the day (daytime or nighttime) and the signal intensity of the CW signal. The

TABLE III
SNR (DB) OF MODIFIED AND UNMODIFIED CW1 AND CW2 SIGNALS (DAEJEON)

	Modified	Unmodified
CW1	21.313	20.9757
CW2	21.877	21.252

TABLE IV
SNR (DB) OF MODIFIED AND UNMODIFIED CW1 AND CW2 SIGNALS (DAESAN)

	Modified	Unmodified
CW1	16.331	14.594
CW2	16.774	15.152

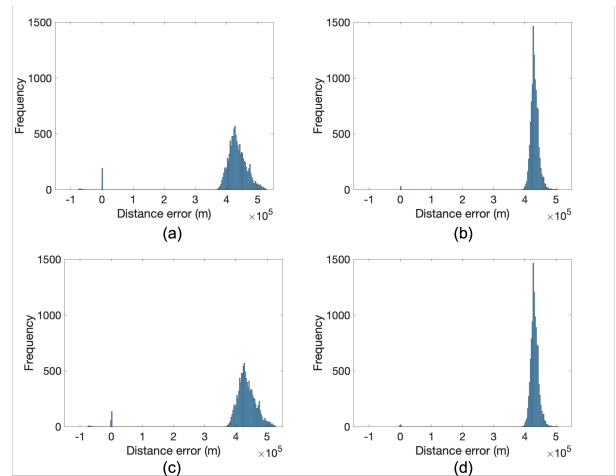


Fig. 3. Range error distribution of (a) modified and (b) unmodified CW1 signal, and (c) modified and (d) unmodified CW2 signal in Daejeon, Korea.

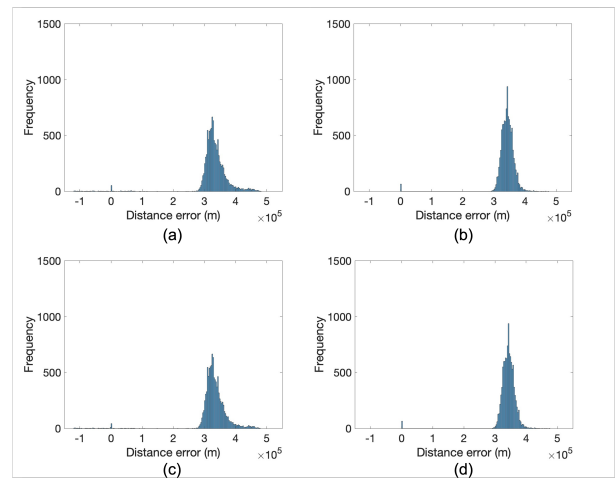


Fig. 4. Range error distribution of (a) modified and (b) unmodified CW1 signal, and (c) modified and (d) unmodified CW2 signal in Daesan, Korea.

results show that the accuracy of measuring the distance during daytime was higher than the case of nighttime, which is due to skywave. Furthermore, this study shows that higher CW signal strength can potentially reduce the influence of skywave.

ACKNOWLEDGMENT

This research was conducted as a part of the project titled “Development of integrated R-Mode navigation system [PMS4440]” funded by the Ministry of Oceans and Fisheries, Republic of Korea (20200450).

REFERENCES

- [1] P. K. Enge, *The Global Positioning System: Signals, Measurements, and Performance*. Springer, 1994.
- [2] K. Park, W. Kim, and J. Seo, “Effects of initial attitude estimation errors on loosely coupled smartphone GPS/IMU integration system,” in *Proc. ICCAS*, 2020, pp. 800–803.
- [3] W. Kim and J. Seo, “Low-cost software-defined GPS simulator with the capability of time synchronization,” in *Proc. ICCAS*, 2018, pp. 1087–1090.
- [4] H. Lee, J. Seo, and Z. Kassas, “Urban road safety prediction: A satellite navigation perspective,” *IEEE Intell. Transp. Syst. Mag.*, 2022, early access.
- [5] K. Park and J. Seo, “Single-antenna-based GPS antijamming method exploiting polarization diversity,” *IEEE Trans. Aerosp. Electron. Syst.*, vol. 57, no. 2, pp. 919–934, Apr. 2021.
- [6] K. Park, D. Lee, and J. Seo, “Dual-polarized GPS antenna array algorithm to adaptively mitigate a large number of interference signals,” *Aerosp. Sci. Technol.*, vol. 78, pp. 387–396, Jul. 2018.
- [7] S. Kim, K. Park, and J. Seo, “Mitigation of GPS chirp jammer using a transversal FIR filter and LMS algorithm,” in *Proc. ITC-CSCC*, 2019.
- [8] E. Schmidt, N. Gatsis, and D. Akopian, “A GPS spoofing detection and classification correlator-based technique using the LASSO,” *IEEE Trans. Aerosp. Electron. Syst.*, vol. 56, no. 6, pp. 4224–4237, Dec. 2020.
- [9] H. Lee, S. Pullen, J. Lee, B. Park, M. Yoon, and J. Seo, “Optimal parameter inflation to enhance the availability of single-frequency GBAS for intelligent air transportation,” *IEEE Trans. Intell. Transp. Syst.*, 2022, early access.
- [10] A. K. Sun, H. Chang, S. Pullen, H. Kil, J. Seo, Y. J. Morton, and J. Lee, “Markov chain-based stochastic modeling of deep signal fading: Availability assessment of dual-frequency GNSS-based aviation under ionospheric scintillation,” *Space Weather*, vol. 19, no. 9, pp. 1–19, Sep. 2021.
- [11] Y. Li, Y. Hua, B. Yan, and W. Guo, “Research on the eLoran differential timing method,” *Sensors*, vol. 20, p. 6518, 2020.
- [12] M. Jia, H. Lee, J. Khalife, Z. M. Kassas, and J. Seo, “Ground vehicle navigation integrity monitoring for multi-constellation GNSS fused with cellular signals of opportunity,” in *Proc. IEEE ITSC*, 2021, pp. 3978–3983.
- [13] S. Jeong, H. Lee, T. Kang, and J. Seo, “RSS-based LTE base station localization using single receiver in environment with unknown path-loss exponent,” in *Proc. ICTC*, 2020, pp. 958–961.
- [14] S. Han, T. Kang, and J. Seo, “Smartphone application to estimate distances from LTE base stations based on received signal strength measurements,” in *Proc. ITC-CSCC*, 2019.
- [15] H. Lee, J. Seo, and Z. Kassas, “Integrity-based path planning strategy for urban autonomous vehicular navigation using GPS and cellular signals,” in *Proc. ION GNSS+*, 2020, pp. 2347–2357.
- [16] J. Rhee and J. Seo, “Low-cost curb detection and localization system using multiple ultrasonic sensors,” *Sensors*, vol. 19, no. 6, Mar. 2019.
- [17] ———, “Ground reflection elimination algorithms for enhanced distance measurement to the curbs using ultrasonic sensors,” in *Proc. ION ITM*, 2018, pp. 224–231.
- [18] E. Kim and J. Seo, “SFOL pulse: A high accuracy DME pulse for alternative aircraft position and navigation,” *Sensors*, vol. 17, no. 10, Sep. 2017.
- [19] S. Lee, E. Kim, and J. Seo, “SFOL DME pulse shaping through digital predistortion for high-accuracy DME,” *IEEE Trans. Aerosp. Electron. Syst.*, vol. 58, no. 3, pp. 2616–2620, June 2022.
- [20] Y. Shin, S. Lee, and J. Seo, “Autonomous safe landing-area determination for rotorcraft UAVs using multiple IR-UWB radars,” *Aerosp. Sci. Technol.*, vol. 69, pp. 617–624, Oct. 2017.
- [21] J. Kim, J.-W. Kwon, and J. Seo, “Simulation study on a method to localize four mobile robots based on triangular formation,” in *Proc. ION Pacific PNT*, 2017, pp. 348–361.
- [22] H. Lee, T. Kang, S. Jeong, and J. Seo, “Evaluation of RF fingerprinting-aided RSS-based target localization for emergency response,” in *Proc. IEEE VTC*, June 2022.
- [23] T. Kang and Y. Shin, “Indoor navigation algorithm based on a smartphone inertial measurement unit and map matching,” in *Proc. ICTC*, 2021, pp. 1421–1424.
- [24] J. A. McEllroy, “Navigation using signals of opportunity in the AM transmission band,” Master’s thesis, Air Force Institute of Technology, 2006.
- [25] P. Wang, Y. Wang, and J. Morton, “Signal tracking algorithm with adaptive multipath mitigation and experimental results for LTE positioning receivers in urban environments,” *IEEE Trans. Aerosp. Electron. Syst.*, 2021, early access.
- [26] C. Huang, H. Qin, C. Zhao, and H. Liang, “Phase - time method: Accurate doppler measurement for iridium NEXT signals,” *IEEE Trans. Aerosp. Electron. Syst.*, pp. 1–9, 2022, early access.
- [27] Y. Yang, J. Khalife, J. J. Morales, and Z. M. Kassas, “Uav waypoint opportunistic navigation in GNSS-denied environments,” *IEEE Trans. Aerosp. Electron. Syst.*, vol. 58, no. 1, pp. 663–678, Feb. 2022.
- [28] G. Johnson, P. Swaszek, J. Alberding, M. Hoppe, and J.-H. Oltmann, “The feasibility of R-Mode to meet resilient PNT requirements for e-Navigation,” in *Proc. ION GNSS*, 2014, pp. 3076–3100.
- [29] G. Johnson and P. Swaszek, “Feasibility study of R-Mode combining MF DGNSS, AIS, and eLoran transmissions,” German Federal Waterways and Shipping Administration, Final Report, Tech. Rep., 2014.
- [30] ———, “Feasibility study of R-Mode using MF DGPS transmissions,” German Federal Waterways and Shipping Administration, Final Report, Tech. Rep., 2014.
- [31] G. W. Johnson, P. F. Swaszek, M. Hoppe, A. Grant, and Šafář, “Initial results of MF-DGNSS R-Mode as an alternative position navigation and timing service,” in *Proc. ION ITM*, 2017, pp. 1206–1226.
- [32] G. Johnson, K. Dykstra, S. Ordell, and P. Swaszek, “R-Mode positioning system demonstration,” in *Proc. ION GNSS*, 2020, pp. 839–855.
- [33] P. F. Swaszek, R. J. Hartnett, and G. W. Johnson, “Ranging/timing off of the NDGPS signal: Potential performance,” in *Proc. ION ITM*, 2012, pp. 452–461.
- [34] S. Jeong and P.-W. Son, “Development of an R-Mode simulator using MF DGNSS signals,” in *Proc. ICCAS*, 2021, pp. 1104–1108.
- [35] P.-W. Son, J. Rhee, J. Hwang, and J. Seo, “Universal kriging for Loran ASF map generation,” *IEEE Trans. Aerosp. Electron. Syst.*, vol. 55, no. 4, pp. 1828–1842, Oct. 2019.
- [36] P.-W. Son, J. Rhee, and J. Seo, “Novel multichain-based Loran positioning algorithm for resilient navigation,” *IEEE Trans. Aerosp. Electron. Syst.*, vol. 54, no. 2, pp. 666–679, Oct. 2018.
- [37] W. Kim, P.-W. Son, S. G. Park, S. H. Park, and J. Seo, “First demonstration of the Korean eLoran accuracy in a narrow waterway using improved ASF maps,” *IEEE Trans. Aerosp. Electron. Syst.*, vol. 58, no. 2, pp. 1492–1496, Apr. 2022.
- [38] J. H. Rhee, S. Kim, P.-W. Son, and J. Seo, “Enhanced accuracy simulator for a future Korean nationwide eLoran system,” *IEEE Access*, vol. 9, pp. 115 042–115 052, Aug. 2021.
- [39] P. Williams and C. Hargreaves, “UK eLoran—Initial operational capability at the Port of Dover,” in *Proc. ION ITM*, 2013, p. 392–402.
- [40] Y. Han, S.-H. Park, G.-C. Seol, T.-H. Kim, and T. H. Fang, “Development of MF R-Mode transmitting system and first broadcast test in R.O.K.,” in *Proc. IPNT*, 2021.
- [41] S. Pasupathy, “Minimum shift keying: A spectrally efficient modulation,” *IEEE Commun. Mag.*, vol. 17, no. 4, pp. 14–22, 1979.
- [42] L. Grundhöfer and S. Gewies, “Ranging/Timing Using the NDGPS Signal,” in *Proc. SDRA*, 2018.
- [43] IEC, “Maritime navigation and radiocommunication equipment and systems - global navigation satellite systems (GNSS) - part 4: Shipborne DGPS and DGLONASS maritime radio beacon receiver equipment - performance requirements, methods of testing and required test results,” International Electrotechnical Commission, International Standard (IEC), Tech. Rep., 2004.